REPORT DOCUMENTATION PAGE

Form Approved
OMB No. 0704-0188

PLEASE DO NOT RETURN YOUR FORM TO THE ABOVE ORGANIZATION.

1. REPORT DATE *(DD-MM-YYYY)*	2. REPORT TYPE	3. DATES COVERED *(From - To)*
31-03-2010	Second Annual and Final Report	March 2008 - March 2010

4. TITLE AND SUBTITLE
Arbitrarily High Order Space-time Method for Conservation Laws on Unstructured Meshes

5a. CONTRACT NUMBER

5b. GRANT NUMBER
FA9550-08-1-0122

5c. PROGRAM ELEMENT NUMBER

6. AUTHOR(S)
Shuangzhang Tu

5d. PROJECT NUMBER

5e. TASK NUMBER

5f. WORK UNIT NUMBER

7. PERFORMING ORGANIZATION NAME(S) AND ADDRESS(ES)
Jackson State University
1400 Lynch St.
Jackson, MS 39217

8. PERFORMING ORGANIZATION REPORT NUMBER

9. SPONSORING/MONITORING AGENCY NAME(S) AND ADDRESS(ES)
Air Force Office of Scientific Research
Computational Mathematics Program
875 North Randolph St.
Arlington, VA 22203

10. SPONSOR/MONITOR'S ACRONYM(S)
AFOSR

11. SPONSOR/MONITOR'S REPORT NUMBER(S)
AFRL-OSR-VA-TR-2012-0863

12. DISTRIBUTION/AVAILABILITY STATEMENT

Distribution A: publicly available

13. SUPPLEMENTARY NOTES

14. ABSTRACT

This research presents a novel high-order space-time method for hyperbolic conservation laws. Two important concepts, the staggered space-time mesh of the space-time conservation element/solution element (CE/SE) method and the local discontinuous basis functions of the space-time discontinuous Galerkin (DG) finite element method, are the two key ingredients of the new scheme. The staggered space-time mesh is constructed using the cell-vertex structure of the underlying spatial mesh. The universal definitions of CEs and SEs are independent of the underlying spatial mesh and thus suitable for arbitrarily unstructured meshes. The solution within each physical time step is updated alternately at the cell level and the vertex level. For this solution updating strategy and the DG ingredient, the new scheme here is termed as the discontinuous Galerkin cell-vertex scheme (DG-CVS). The high order of accuracy is achieved by employing high-order Taylor polynomials as the basis functions inside each SE. Quadrature-free integration is implemented to improve efficiency. The present DG-CVS exhibits many distinct features such as Riemann-solver-free, high-order accuracy in both space and time, point-implicitness, compactness, and ease of handling boundary conditions.

15. SUBJECT TERMS
Conservation laws, space time method, cell vertex scheme, high order method.

16. SECURITY CLASSIFICATION OF:			17. LIMITATION OF ABSTRACT	18. NUMBER OF PAGES	19a. NAME OF RESPONSIBLE PERSON
a. REPORT	b. ABSTRACT	c. THIS PAGE			Shuangzhang Tu
U	U	U	UU	13	19b. TELEPHONE NUMBER *(Include area code)* (601) 979-1275

Reset

Arbitrarily High Order Space-time Method for Conservation Laws on Unstructured Meshes

Second Annual and Final Report to AFOSR
regarding AFOSR Grant Number FA9550-08-1-0122

Shuangzhang Tu
Department of Computer Engineering
Jackson State University, Jackson, Mississippi

1 Foreword

This report first reviews our accomplishments on the research under AFOSR Grant FA9550-08-1-0122 in the second year (March 15, 2009 - March 14, 2010), and then reviews the comprehensive accomplishments over the entire project period (Mach 15, 2008 - March 14, 2010). Therefore, this report also serves as the Final Report.

The high-order space time method proposed in this research has been termed as the discontinuous Galerkin Cell-Vertex Scheme (DG-CVS) for its DG ingredient and its alternate cell vertex solution updating strategy.

2 Accomplishments in the second year

In the second year, the effort addressed the following issues:

1. *Solution limiting procedure.* The limiting procedure performs as an alternative method to limit (or remap) high order but oscillatory solutions across discontinuities, thus maintaining the stability of DG-CVS. In the present approach, limiting is active only in truly oscillatory regions detected by a reliable oscillation indicator. Since the limiter must be conservative, the solution is reformulated in terms of the cell average and cell-averaged solution derivatives, and the limiter limits the averaged solution derivatives only while preserving the cell average. The limiter ensures the solution satisfies the following two constraints: (i) the solution does not exceed the maximum or minimum cell averages in the local stencil; and (ii) the solution gradient is consistent with the local solution variation across each edge. The limiting procedure is recast as a quadratic programming problem with linear inequality constraints, which can be solved by the active set method. It is hoped that through the quadratic programming, the optimum limiting factors can be obtained while satisfying the linear constraints. For high order solutions, these constraints are formulated as the *sufficient* (not necessary) conditions. The method seems to work fine for 1-D equations (systems) and extension to higher dimensions still needs more work.

2. *Employing the quadruple precision arithmetic via MPACK* [1]. The purpose of doing this is to verify that the DG-CVS is truly *arbitrarily* high-order accurate as long as the linear system resulted from discretization can be accurately solved. In the current implementation, Taylor polynomials are used as the basis functions and Taylor polynomials are notorious in generating severely ill-conditioned systems. Therefore, double-precision arithmetic cannot reliably solve the system when the degree (p) of basis polynomials is high ($p > 4$). The quadruple precision arithmetic provided by MPACK is able to solve highly ill-conditioned systems and verifies that optimal convergence rate, $p + 1$, can be reached for $p > 4$.

3. *Improving the efficiency of the present high-order space-time method by implementing it on the overset Cartesian/quadrilateral grids.* Though the DG-CVS is designed for arbitrarily unstructured grids, rectangular/quadrilateral grids are superior to triangular grids in terms of efficiency. The body-fitted quadrilateral mesh is used to wrap the object and the Cartesian grid serves as the background mesh. The contact boundary extracted from the quadrilateral mesh is used to determine the overlapping region between the two meshes. The overlapping region is kept minimum but large enough to transfer solutions between the two meshes. The Cartesian mesh around the overlapping region is geometrically refined to match the resolution of the corresponding quadrilateral mesh. The portion of the Cartesian mesh covered by the quadrilateral mesh and the object and beyond the the overlapping region is discarded. The inter-mesh solution transfer strategy is crucial in ensuring the global flux conservation. The donor cell is the cell on the counterpart mesh where the receptor cell is located. A simple test of a subsonic flow around a circular cylinder demonstrates that the current implementation is quite successful.

4. *Dissemination via conference and publications.* The limiting procedure described above has been presented and published (AIAA Paper 2009-3983) in the 19th AIAA Computational Fluid Dynamics Conference, June, 2009, San Antonio, TX. The results of the implementation on overset Cartesian/quadrilateral grids have been presented and published (AIAA Paper 2010-0544) in the 48th AIAA Aerospace Science Meeting, January 2010 in Orlando, Florida. A revised comprehensive paper is to appear in *Communications in Computational Physics.*

3 Accomplishments in the entire grant period

Over the entire grant period, the present high-order space time method, which is termed as the discontinuous Galerkin cell-vertex scheme (DG-CVS), has been verified and developed for both scalar advection equations and compressible Euler equations. The work so far shows that DG-CVS is a promising method for hyperbolic conservation laws. The most distinct features of the DG-CVS can be summarized as:

- locally and globally space-time flux conservative.
- alternate solution updating at the cell level and the vertex level within each physical time step.
- Riemann-solver-free for advection problem.
- high-order accurate in both space and time.
- highly compact regardless of the order.

- suitable for arbitrarily unstructured meshes.
- simple boundary condition treatment.

A comprehensive list of accomplishments is given below:

1. *Alternate cell vertex solution updating strategy.* Inspired by the space-time conservation element/solution element (CE/SE) method [2], space-time flux conservation is enforced over staggered space-time conservation elements. In this research universal definitions of CEs and SEs using the cell-vertex structure of the underlying spatial mesh are utilized such that the method is suitable for arbitrarily unstructured meshes. The solution within each physical time step is updated alternately at the cell level and the vertex level. This strategy circumvents the need of using Riemann solvers to provide the inter-cell fluxes and leads to a Riemann-solver-free solver.

2. *Arbitrarily high-order accuracy in both space and time.* The high order of accuracy is achieved by employing high-order polynomials basis functions inside each SE, as in the discontinuous Galerkin (DG) method [3]. What is different from the classic DG method is that no any type of Riemann solvers is used for the inter-cell flux thanks to the cell vertex solution updating strategy explained above. This DG ingredient also makes the current method deviate from the CE/SE method by providing high order accuracy. For the DG ingredient and the cell-vertex solution updating strategy, the new scheme here is termed as the discontinuous Galerkin cell-vertex scheme (DG-CVS).

3. *Formulation.* Considering the following one dimension linear scalar advection equation

$$\frac{\partial u(x,t)}{\partial t} + \frac{\partial f(u)}{\partial x} = 0 \tag{1}$$

where u is the advected quantity and f is the flux. The approximate solution u^h is sought within each space-time solution element (SE), denoted as K. When restricted to the SE, u^h belongs to the finite dimensional space $\mathcal{U}(K)$ such that

$$u^h(x,t) = \sum_{j=1}^{N} \phi_j s_j \tag{2}$$

where $\{\phi_j\}_{j=1}^N$ are some type of polynomial basis functions, $\{s_j\}_{j=1}^N$ are the unknowns to be determined and N is the number of basis functions depending on the degree of the polynomial function.
According to Galerkin orthogonality, one can multiply the governing equation with each of the basis functions $\{\phi_i\}_{i=1}^N$ to obtain

$$\int_\Omega \phi_i \left(\frac{\partial u^h}{\partial t} + \frac{\partial f^h}{\partial x} \right) \mathrm{d}\Omega = 0 \quad \text{for } i = 1, \cdots, N \tag{3}$$

where Ω is the conservation element (CE) corresponding to the solution element K.
Integrating the resulting weak form by parts yields

$$\int_\Omega \left[\frac{\partial \phi_i}{\partial t} u^h + \frac{\partial \phi_i}{\partial x} f^h \right] \mathrm{d}\Omega = \int_\Gamma \phi_i F^h_{\mathbf{n}} \mathrm{d}\Gamma \tag{4}$$

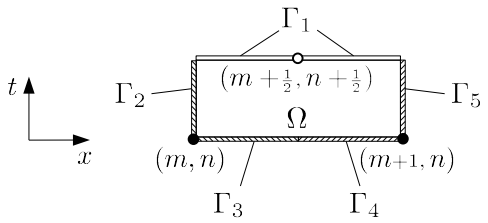

Figure 1: Illustration of space-time flux conservation in a conservation element at the cell level.

where

$$F^h_{\mathbf{n}} = F^h \cdot \mathbf{n} = \left(f^h,\, u^h\right) \cdot (n_x, n_t) \tag{5}$$

is the space-time flux normal to the boundary of the space-time CE. $\mathbf{n} = (n_x, n_t)$ is the outward unit normal of the CE boundary. $\Gamma = \partial\Omega$ is the boundary of the CE under consideration.

The cell level CE shown in Fig. 1 is taken as a specific example here. As shown in Fig. 1, divide Γ into five sections Γ_1, Γ_2, Γ_3, Γ_4 and Γ_5 where Γ_1 belongs to the SE associated with $(m+\frac{1}{2}, n+\frac{1}{2})$ where the solution is being sought, Γ_2 and Γ_3 the SE associated with (m,n) and Γ_4 and Γ_5 the SE associated with $(m+1,n)$. Note that the solutions at nodes (m,n) and $(m+1,n)$ are known since they are at the previous time level. Considering the outward unit normal of each boundary, Eq. (4) becomes

$$\begin{aligned} &\int_\Omega \left[\frac{\partial \phi_i}{\partial t} u^h_{m+\frac{1}{2},n+\frac{1}{2}} + \frac{\partial \phi_i}{\partial x} f^h_{m+\frac{1}{2},n+\frac{1}{2}}\right] \mathrm{d}\Omega - \int_{\Gamma_1} \phi_i u^h_{m+\frac{1}{2},n+\frac{1}{2}} \mathrm{d}\Gamma \\ &= \int_{\Gamma_2} \phi_i F^h_{\mathbf{n}(m,n)} \mathrm{d}\Gamma - \int_{\Gamma_3} \phi_i u^h_{m,n} \mathrm{d}\Gamma - \int_{\Gamma_4} \phi_i u^h_{m+1,n} \mathrm{d}\Gamma + \int_{\Gamma_5} \phi_i F^h_{\mathbf{n}(m+1,n)} \mathrm{d}\Gamma \end{aligned} \tag{6}$$

which leads to a linear or nonlinear equation system (depending on whether f is a linear or nonlinear function of u) that can be solved for the unknown $u^h_{m+1/2,n+1/2}$ at the space-time node $(m+1/2, n+1/2)$.

4. *Choice of basis polynomials.* In this project, Taylor polynomials are chosen as the basis functions for three reasons. First, the Taylor polynomial has no restrictions on the geometric shape of the conservation element (SE). The SE can be of arbitrary shape which is typically polygonal cylinder on spatially unstructured meshes . By contrast, Lagrange polynomials are only well defined on simplicial elements or elements allowing tensor products, and Chebyshev polynomials and Legendre polynomials are only well defined on elements allowing tensor products.
   Second, with Taylor polynomials, the basis functions are polynomials with respect to the physical coordinates Δx and Δt. Other polynomials usually define the basis function using reference coordinates (e.g., ξ and η). The numerical integration involves the derivatives of the basis function with respect to the physical coordinates. With Taylor polynomials, the derivatives can be directly obtained by taking the derivative of the basis functions with respect to Δx and Δt without resorting to the chain rule as is required when other polynomials are employed.
   Third, the derivatives of Taylor polynomials are a lower order subset of the original Taylor polynomials. This allows efficient implementation when evaluating integrals involving products of polynomials.

The above discussions of the advantages of Taylor polynomials over other polynomials are completely based on the implementation point of view. One should keep in mind that high degree Taylor polynomials are notorious in generating severely ill-conditioned systems. It is well known that the number of reliable digits of the solution of linear systems is related to the conditioning of the system. As a result, high degree Taylor polynomials are expected to yield inaccurate solutions due to the ill conditioning of the system. Therefore, choosing Taylor polynomials is not wise from the accuracy point of view. However, the goal of this research is to demonstrate the efficacy of the DG-CVS idea, so Taylor polynomials are employed for quick implementation.

5. *Insensitivity to Courant number when using high-order basis polynomials.* It is well known that some space-time and fully discrete methods exhibits excess dissipation when the time step is vanishingly small. The present study shows that the present DG-CVS $p1$ case exhibits similar phenomenon, namely, when the time step is vanishingly small, the accuracy is degraded. However, for higher degrees, the DG-CVS is less and less sensitive to small Courant numbers. Actually, in the case of $p4$, a slightly higher accuracy is obtained when a smaller time step is used.

6. *Quadrature-free implementation.* The DG-CVS formulation involves both surface and volume integrals. If the underlying spatial mesh is unstructured, the vertex-level CEs are general polygonal cylinders containing general polygonal bases and quadrilateral side faces where the Gaussian quadrature rule cannot be directly applied. In addition, even for purely rectangular meshes where the Gaussian quadrature rule can be applied to all integrals, integration by quadrature rule is prohibitively expensive, especially in high dimensions. Therefore, quadrature-free implementation is sought in the research to improve the efficiency of the method. We can combine the divergence theorem and indefinite integration to transform a volume integral to surface integrals and further to line integrals. Finally, analytical formulae are available to evaluate the line integrals. Numerical experiments show that the quadrature-free implementation drastically increases the efficiency by a factor of 60 for the case of $p = 4$.

7. *Boundary condition treatment.* The space-time formulation makes it simple to implement the Dirichlet and Neumann boundary conditions. The boundary conditions are accounted for by modifying the resulting linear equation system from discretization. Both the left hand side matrix and right hand side vector are modified consistently. For the outflow boundary condition, nothing needs to be modified as long as the matrix is formed by taking into account the contribution from the outer side face of the boundary CE.

8. *Accuracy for linear scalar advection equations (one dimension or two dimensions).* In linear advection equations, the flux satisfies the same polynomial distribution as the solution itself scaled by a constant advection speed. If the solution inside the conservation element is assumed to satisfy a polynomial of degree p, then the order of accuracy should be $p+1$. This has been confirmed in the grid convergence study for both 1-D and 2-D problems. The convergence rates are truly optimal $p + 1$ as long as the equation system resulted from discretization can be solved accurately. When $p > 4$, the system becomes highly ill-conditioned due to the use of Taylor polynomial bases. Therefore, quadruple precision arithmetic is required to obtain the optimal convergence rate when p is high.

9. *Accuracy for nonlinear scalar advection equations (one dimension or two dimensions).* In nonlinear advection equations (e.g., inviscid Burgers equation), the flux is a nonlinear function of the solution. Therefore, the flux satisfies a different polynomial distribution than the

$\|\|\text{error}\|\|_\infty$ under different Courant number				
Courant number $\sigma = \|a\|\delta t/\delta x$	$p1$	$p2$	$p3$	$p4$
0.2	3.31E-02	1.42E-04	2.62E-05	4.12E-07
0.02	1.82E-01	3.18E-04	2.63E-05	2.42E-07
0.002	8.20E-01	3.14E-03	2.83E-05	2.08E-07

Table 1: Sensitivity to the Courant number of the present method.

solution itself. Thanks to the quadrature-free implementation, the integral involving the flux can be evaluated exactly. The grid convergence study shows that the optimal convergence rate of the solution can also be reached for inviscid 1-D and 2-D Burgers equations.

10. *Accuracy on unstructured triangular meshes.* The grid convergence study has also been conducted on unstructured triangular meshes. Again, optimal convergence rate can be reached for each p.

11. *Extension to compressible Euler equations (one dimension or two dimensions).* The DG-CVS idea can be directly applied to more complex hyperbolic compressible Euler equations. In our implementation, following Lowrie et al. [4], we choose the working variables to be

$$\mathbf{Q} = [\sqrt{\rho},\ \sqrt{\rho}u,\ \sqrt{\rho}v,\ \sqrt{\rho}H]^{\mathrm{T}} \tag{7}$$

where ρ, u, v, H are density, x- and y-velocity components, and specific total enthalpy, respectively. By choosing such working variables, all components of the conservative state vector and flux vectors can be expressed as the *double product* between working variables, which is analogous to the inviscid Burger's equation.

12. *Solution limiting procedure.* This has been explained in the section of "Accomplishments in the second year".

13. *Quadruple precision implementation.* This has been explained in the section of "Accomplishments in the second year".

14. *Implementation on overset Cartesian/quadrilateral meshes.* This has been explained in the section of "Accomplishments in the second year".

4 Numerical illustrations

This section presents some numerical results to illustrate the findings listed in sections 2 and 3.

Table 1 lists the ∞-errors of $p1$, $p2$, $p3$ and $p4$ cases when various Courant numbers are used for a linear advection equation.

Figure 2 shows the convergence order of the DG-CVS. It can be seen that the optimal rate, $p+1$, can be reached for all p (degree of the basis polynomial). Note that the $p5$ and $p6$ cases are run using the quadruple precision arithmetic due to the ill-conditioning caused by Taylor polynomials. Figure shows similar phenomenon for nonlinear inviscid Burgers equation. Figures 4 and 5 show

Table 2: Order of accuracy for the 1-D linear sinusoidal wave advection at $t = 1.0$. Quadruple precision.

p	n_c	l_1 error	order	l_∞ error	order
4	10	2.80E-07	-	4.12E-07	-
	20	8.18E-09	5.096	1.25E-08	5.037
	40	2.46E-10	5.057	3.81E-10	5.041
	80	7.48E-12	5.039	1.17E-11	5.029
	160	2.32E-13	5.013	3.63E-13	5.008
5	10	1.31E-08	-	2.19E-08	-
	20	2.14E-10	5.933	3.53E-10	5.960
	40	3.42E-12	5.967	5.51E-12	6.001
	80	5.39E-14	5.986	8.58E-14	6.004
	160	8.44E-16	5.999	1.33E-15	6.007
6	10	2.00E-11	-	2.95E-11	-
	20	1.43E-13	7.129	2.16E-13	7.094
	40	1.06E-15	7.072	1.64E-15	7.039
	80	8.18E-18	7.022	1.28E-17	7.009
	160	6.38E-20	7.003	9.98E-20	6.997

Table 3: Order of accuracy for the 1-D inviscid Burgers equation at $t = 0.12$. Quadruple precision.

p	n_c	$\bar{n}_{\text{iter}}$	l_1 error	order	l_∞ error	order
4	10	5.45	5.57E-06	-	2.16E-05	-
	20	5.00	1.79E-07	4.958	8.31E-07	4.703
	40	4.93	8.09E-09	4.469	4.30E-08	4.270
	80	4.82	2.47E-10	5.032	1.60E-09	4.750
	160	4.56	7.60E-12	5.023	5.31E-11	4.912
5	10	5.64	1.44E-06	-	6.93E-06	-
	20	5.21	1.84E-08	6.296	1.16E-07	5.905
	40	4.98	5.33E-10	5.108	6.81E-09	4.086
	80	4.89	9.86E-12	5.756	1.18E-10	5.848
	160	4.74	1.67E-13	5.882	1.89E-12	5.968
6	10	5.61	4.98E-07	-	1.80E-06	-
	20	5.30	6.82E-09	6.188	3.23E-08	5.799
	40	4.96	5.87E-11	6.862	3.55E-10	6.510
	80	4.90	5.15E-13	6.832	4.46E-12	6.312
	160	4.77	4.61E-15	6.803	4.63E-14	6.592

Table 4: Order of accuracy for the 2-D linear sinusoidal wave advection at $t = 1.0$ on unstructured triangular meshes.

p	mesh size (h)	l_1 error	order	l_∞ error	order
1	0.2	5.21E-02	-	1.07E-01	-
	0.1	9.14E-03	2.51	2.01E-02	2.41
	0.05	1.70E-03	2.43	3.97E-03	2.34
	0.025	3.48E-04	2.29	8.37E-04	2.25
	0.0125	7.71E-05	2.17	1.91E-04	2.13
2	0.2	4.68E-04	-	1.90E-03	-
	0.1	4.06E-05	3.53	2.94E-04	2.69
	0.05	3.88E-06	3.39	3.60E-05	3.03
	0.025	4.09E-07	3.25	4.46E-06	3.01
	0.0125	4.60E-08	3.15	5.60E-07	2.99
3	0.2	7.05E-05	-	2.77E-04	-
	0.1	4.48E-06	3.98	1.76E-05	3.98
	0.05	2.84E-07	3.98	1.11E-06	3.99
	0.025	1.80E-08	3.98	6.96E-08	4.00
4	0.2	1.91E-06	-	8.61E-06	-
	0.1	5.79E-08	5.04	2.80E-07	4.94
	0.05	1.75E-09	5.05	9.41E-09	4.90
	0.025	5.39E-11	5.02	3.18E-10	4.89

Table 5: Order of accuracy for the 2-D inviscid Burgers equation at $t = 0.075$ on unstructured triangular meshes.

p	mesh size (h)	$\bar{n}_{\text{iter}}$	l_1 error	order	l_∞ error	order
1	0.2	3.39	2.12E-02	-	9.92E-02	-
	0.1	3.53	5.58E-03	1.93	2.79E-02	1.83
	0.05	3.18	1.40E-03	1.99	7.26E-03	1.94
	0.025	2.95	3.46E-04	2.02	1.75E-03	2.05
	0.0125	2.96	8.59E-05	2.01	4.26E-04	2.04
2	0.2	3.38	7.50E-04	-	1.14E-02	-
	0.1	3.55	1.03E-04	2.86	1.73E-03	2.72
	0.05	3.17	1.19E-05	3.11	2.60E-04	2.73
	0.025	2.94	1.21E-06	3.30	4.21E-05	2.63
	0.0125	2.97	1.28E-07	3.24	7.14E-06	2.56
3	0.2	3.52	4.35E-04	-	6.34E-03	-
	0.1	3.64	3.47E-05	3.65	3.85E-04	4.04
	0.05	3.29	2.42E-06	3.84	4.00E-05	3.27
	0.025	2.95	1.52E-07	3.99	2.73E-06	3.87
	0.0125	2.97	9.55E-09	3.99	1.67E-07	4.03
4	0.2	3.58	6.10E-05	-	7.15E-04	-
	0.1	3.62	2.71E-06	4.49	3.82E-05	4.23
	0.05	3.26	8.18E-08	5.05	1.77E-06	4.43
	0.025	2.94	2.36E-09	5.12	8.07E-08	4.46

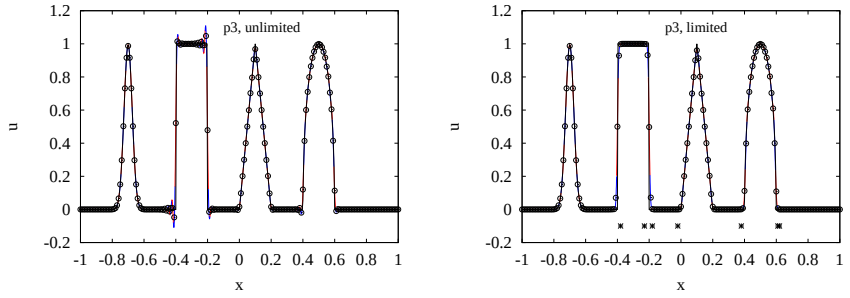

(a) (b)

Figure 2: Illustration of solution limiting.

Table 6: Comparison of the time cost in integration using the Gaussian quadrature rule and quadrature-free approach.

		Scaled time cost			
		$p1$	$p2$	$p3$	$p4$
Compute M_{ij} contributions from the top face of CEs	*Gaussian quadrature*	0.99	1.26	2.08	4.34
	Quadrature-free	1	1	1	1
Compute M_{ij} contributions from the volume of CEs	*Gaussian quadrature*	1.78	5.64	24.48	60.38
	Quadrature-free	1	1	1	1

the convergence orders of 2-D linear and nonlinear advection equations on unstructured triangular meshes.

Figure 2 illustrates the performance of solution limiting.

Figure 3 shows the boundary condition treatment of inflow and outflow boundary conditions.

Table 6 illustrates the cost saving using the quadrature-free implementation compared to the Gaussian quadrature integration.

Figures 4, 5 and 6 present some results for compressible Euler equations including the 1-D shock tube problem, 2-D isentropic vortex advection problem and the forward-facing step problem.

Figure 7 shows the simulated pressure field on an overset Cartesian/quadrilateral mesh of a subsonic flow around a circular cylinder.

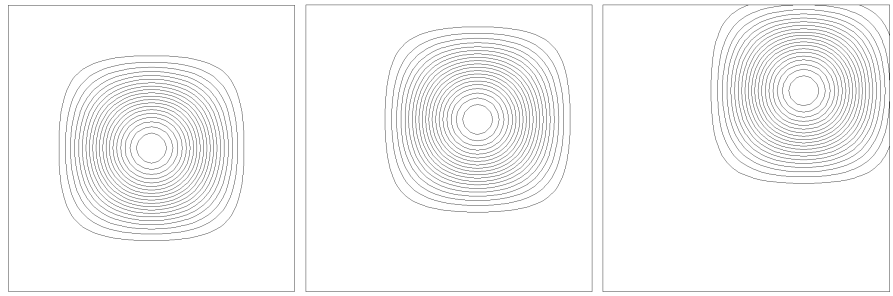

(a) $t = 0.0$ (b) $t = 0.2$ (c) $t = 0.4$

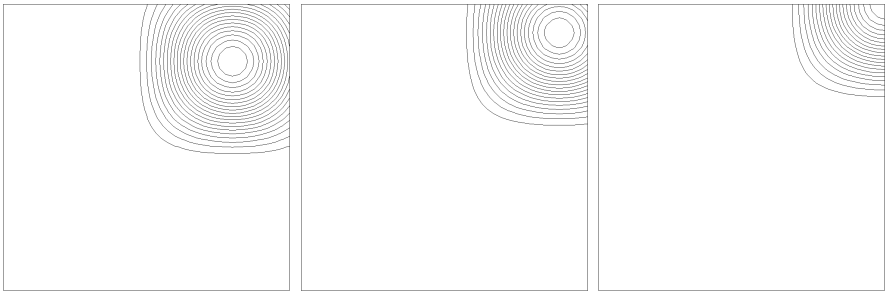

(d) $t = 0.6$ (e) $t = 0.8$ (f) $t = 1.0$

Figure 3: Advection of a doubly raised cosine surface. $p2$ solution on 40×40 rectangular mesh.

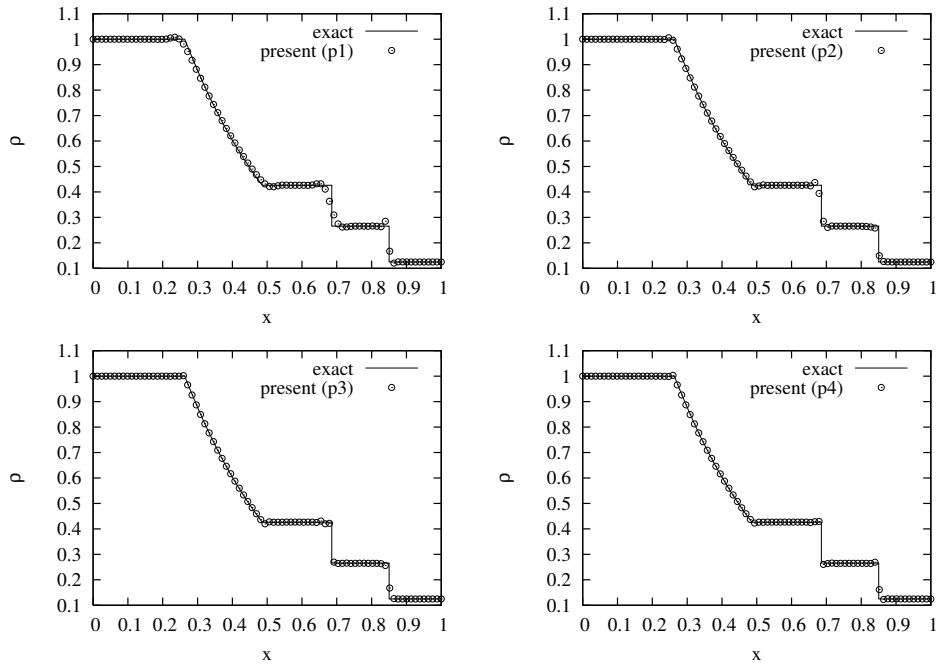

Figure 4: Density distribution of the 1-D shock tube problem at $t = 0.2$ when various degrees of basis polynomials employed. Without limiter.

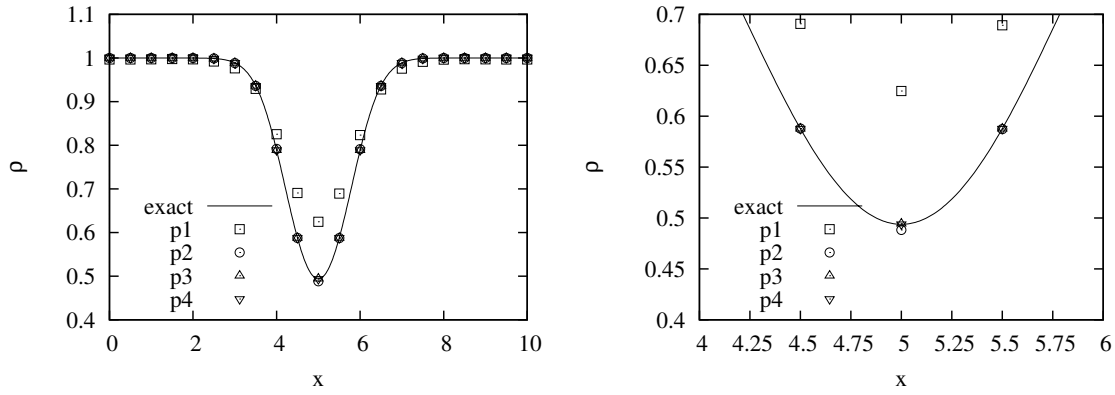

Figure 5: Advection of isentropic vortex on a 20×20 rectangular mesh. Comparison of density accuracy between $p1 - p4$ cases. The close-up view is on the right.

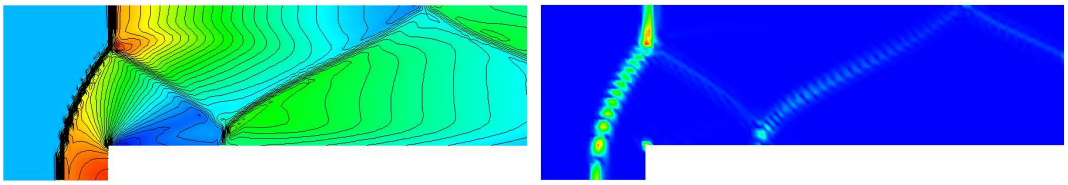

Figure 6: Solution of a supersonic ($M = 3$) flow through a channel with forward-facing step at $t = 4.0$. Without limiter. Left: $p1$ density field. Right: residual of the continuity equation.

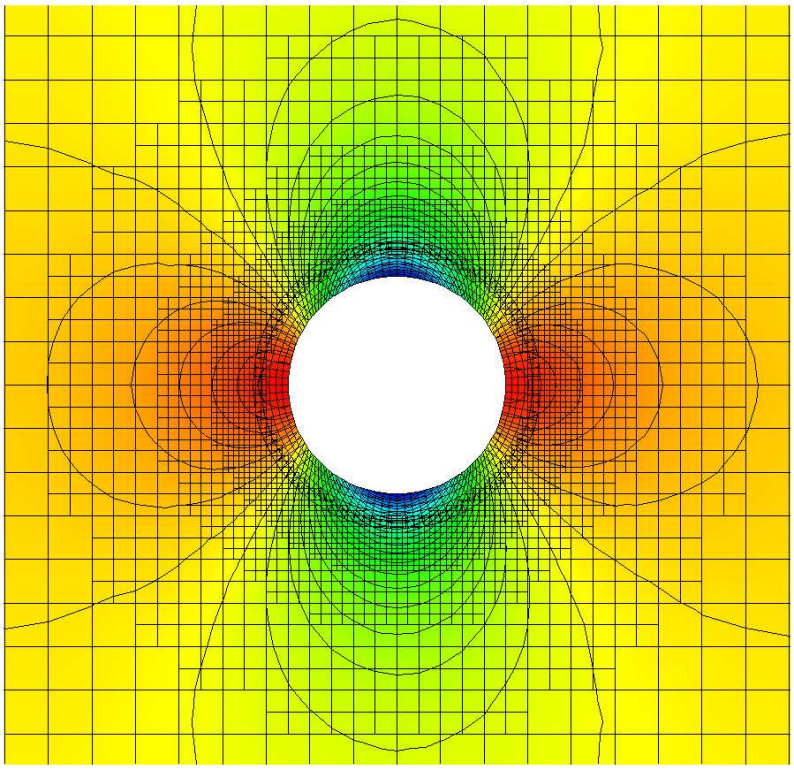

Figure 7: Steady pressure field the inviscid flow ($M = 0.1$) passing around a circular cylinder.

5 References

1. M. Nakata. The MPACK: Multiple precision arithmetic BLAS (MBLAS) and LAPACK (MLAPACK), 2009. http://mplapack.sourceforge.net/.
2. S.-C. Chang and W. To. A new numerical framework for solving conservation laws: the method of space-time conservation element and solution element, 1991. *NASA TM 1991-104495*.
3. B. Cockburn and C.-W. Shu. Runge-Kutta discontinuous Galerkin methods for convection dominated problems. *J. Sci. Comput.*, 16(3):173–261, 2001.
4. R. Lowrie, P. Roe, and B. van Leer. A space-time discontinuous Galerkin method for the time-accurate numerical solution of hyperbolic conservation laws, 1995. AIAA Paper 1995-1658.

6 Acknowledgment/Disclaimer

This work was sponsored by the Air Force Office of Scientific Research under grant number FA9550-08-1-0122. The views and conclusions contained herein are those of the author and should not be interpreted as necessarily representing the official policies or endorsements, either expressed or implied, of the Air Force Office of Scientific Research or the U.S. Government.

7 Publications

1. S. Tu, "A High-order Space-time Method for Compressible Euler Equations," AIAA Paper 2009-1335, 2009.
2. S. Tu, "A Solution Limiting Procedure for a High Order Space-Time Method," AIAA Paper 2009-3983, 2009.
3. S. Tu and Z. Tian, "Preliminary Implementation of a High Order Space-time Method on Overset Cartesian/Quadrilateral Grids," AIAA Paper 2010-0544, 2010.
4. S. Tu, G. Skelton and Q. Pang, "A Compact High-order Space-time Method for Conservation Laws," to appear in *Communications in Computational Physics*, 2010.

8 Personnel supported

- Shuangzhang Tu, assistant professor (PI).
- Ziyu Tian, graduate student.
- Venugopal Reddy Peddireddy, undergraduate student.
- Praveen Kumar Gampala, graduate student.
- Mahmoud Ibrahim, graduate student.

9 AFOSR point of contact

Dr. Fariba Fahroo, Program Manager, Computational Mathematics, AFOSR/NL, 875 North Randolph Street Suite 325, Room 3112 Arlington, VA 22203, (703) 696-8429, Fax (703) 696-8450, DSN 426-8429, `fariba.fahroo@afosr.af.mil`.

10 Interactions/transitions

Conference presentations:

1. 47th AIAA Aerospace Science Meeting, January, 2009, Orlando, FL. (speaker: S. Tu).
2. 19th AIAA Computational Fluid Dynamics Conference, June, 2009, San Antonio, TX. (speaker: S. Tu).
3. 48th AIAA Aerospace Science Meeting, January, 2010, Orlando, FL. (speaker: S. Tu).

11 Changes in research objectives

None.

12 Change in AFOSR program manager

None.

13 Extensions granted or milestones slipped

None.

14 New discoveries

None patentable.